



ELSEVIER

1 April 2002

Optics Communications 204 (2002) 99–106

OPTICS
COMMUNICATIONS

www.elsevier.com/locate/optcom

Space and spectral behaviour of optical systems under broadband illumination by using a Wigner distribution function approach

Dobryna Zalvidea^{a,*}, Sergio Granieri^{a,1}, Enrique E. Sicre^b

^a *Centro de Investigaciones Opticas (CIOp), C. Correo 124, (1900) La Plata, Argentina*

^b *Faculty of Engineering, Universidad Argentina de la Empresa (UADE), Lima 717, (1073) Buenos Aires, Argentina*

Received 9 May 2001; received in revised form 6 November 2001; accepted 30 January 2002

Abstract

The on-axis image irradiance obtained from a radially symmetric optical system under broadband illumination is analysed in the phase-space domain of the Wigner distribution function associated with a modified one-dimensional pupil aperture. To this end, a coordinate transformation is employed in such a way that the varying on-axis irradiance can be derived from different slices of a two-dimensional Wigner distribution function, which involve both the defocus distance and the dispersion properties of the optical system. The method is illustrated by comparing the imaging performance of four different pupil apertures, when the system is illuminated with a light beam having a gaussian spectral content. © 2002 Published by Elsevier Science B.V.

Keywords: Optical imaging systems; Broadband illumination; Wigner distribution function

1. Introduction

The analysis of the imaging performance of optical systems under monochromatic illumination using phase-space signal representations, like the Wigner distribution function (WDF) or the ambiguity function, has been proved to be a useful tool for different applications [1–14]. Image quality parameters defined either in the image space, such as the normalised irradiance or Strehl ratio, or in

the spatial frequency domain, such as the optical transfer function, can be conveniently treated in the phase-space domain. The properties of different pupil transmittance functions, suffering aberrations and/or defocusing, can be investigated through a two-dimensional WDF associated with a modified pupil function derived from the original one by performing a coordinate change that takes into account the pupil symmetry [13].

In this paper we extend the WDF treatment of optical imaging systems to take into account polychromatic or broadband illumination. In this way, the Kirchhoff–Fresnel solution to the wave equation should include the dispersion phase terms that appear due to the wavenumber frequency

* Corresponding author. Fax: +54 221 471 2771.

E-mail address: dobrynaz@ciop.unlp.edu.ar (D. Zalvidea).

¹ Present address: Department of Physics and Applied Optics, Rose Hulman Institute of Technology, Terre Haute, IN, USA.

dependence. From this expression, the on-axis image irradiance is obtained for the particular case of radially symmetric pupil functions. A relationship is derived which links this irradiance with phase-space projections along vertical slices of the two-dimensional WDF associated with the modified pupil function. Thus, the combined spatial/spectral behaviour of the optical system can be visualised in the phase-space, as e.g., the well-known chromatic focal shift that takes place with broadband illumination. Finally, the approach is illustrated by comparing the imaging performance of four pupil functions: the circular uniform aperture, the annular aperture, the hyper-gaussian amplitude transmission function and a quartic phase pupil mask. It is found that a better performance to defocusing is exhibited by the two latter apertures, for the case of a illumination beam having a gaussian spectral content.

2. Basic theory

For analysing the spatial and temporal properties of the light field amplitude in the neighbourhood of the focal and/or image planes, it should be solved the Helmholtz equation in the frequency domain, i.e.,

$$[\nabla^2 + k^2(\omega)]U(\vec{r}; \omega) = 0, \quad (1)$$

where ∇^2 is the Laplacian operator, $k(\omega)$ is the wavenumber which depends on the temporal frequency ω , and U is the scalar field amplitude. If we consider a plane wave as the incident light beam of the optical imaging system (see Fig. 1), the solution of Eq. (1) for the image space, in the framework of the Fresnel–Kirchhoff theory, can be written as

$$\begin{aligned} U(r, \theta, z; \Delta\omega) &= KA(\Delta\omega)e^{ik_0 n_0 e \Delta\omega(a_1 + a_2 \Delta\omega)} \\ &\times \exp\left\{i \frac{k_0}{2(f_0 + z)} \left(1 + \frac{\Delta\omega}{\omega_0}\right) r^2\right\} \\ &\times \int_0^\infty \int_0^{2\pi} P_0(\rho, \phi) e^{i\Phi(\rho, \phi)} \\ &\times \exp\left\{-\frac{ik_0}{2f_0} \left(1 - \frac{f_0}{f_0 + z}\right) \rho^2\right\} \\ &\times \exp\left\{-\frac{ik_0 \Delta\omega}{2f_0} \left(a'_1 + a'_2 \Delta\omega - \frac{f_0}{\omega_0(f_0 + z)}\right) \rho^2\right\} \\ &\times \exp\left\{-\frac{ik_0}{(f_0 + z)} \left(1 + \frac{\Delta\omega}{\omega_0}\right) r \rho \cos(\phi - \theta)\right\} \rho d\rho d\phi, \end{aligned} \quad (2)$$

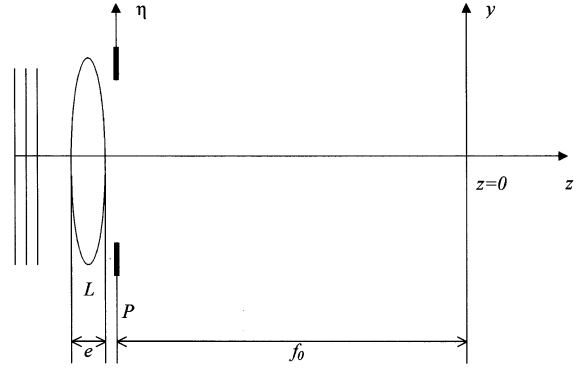


Fig. 1. Scheme of the optical imaging system.

where K is a complex constant; $A(\Delta\omega)$ is the spectral distribution content of the illuminating beam, centred at $\omega = \omega_0$, as a function of the difference variable $\Delta\omega = \omega - \omega_0$; e is the thickness of the lens along the optical axis; $k_0 = \omega_0/c$ and $n_0 = n(\omega_0)$ are the wavenumber in air and the refractive index of the lens material, respectively, both calculated for $\omega = \omega_0$. In Eq. (2), the field amplitude is expressed in polar coordinates (r, θ) , being z the axial distance taken from the focal point $z = 0$. Besides, $P_0(\rho, \phi)$ and $\Phi(\rho, \phi)$ are the amplitude transmittance and the phase distribution associated with the pupil function P , expressed in polar coordinates (ρ, ϕ) . The remainder parameters involved in Eq. (2), which take into account the material dispersion up to the second order, are

$$a_1 = \frac{1}{\omega_0} + \frac{1}{n_0} \left. \frac{dn(\omega)}{d\omega} \right|_{\omega_0}, \quad (3.1)$$

$$a_2 = \frac{1}{n_0 \omega_0} \left. \frac{dn(\omega)}{d\omega} \right|_{\omega_0} + \frac{1}{2n_0} \left. \frac{d^2n(\omega)}{d\omega^2} \right|_{\omega_0}, \quad (3.2)$$

$$a'_1 = \frac{1}{\omega_0} + \frac{1}{n_0 - 1} \left. \frac{dn(\omega)}{d\omega} \right|_{\omega_0}, \quad (3.3)$$

$$\begin{aligned} a'_2 &= \frac{1}{(n_0 - 1)\omega_0} \left. \frac{dn(\omega)}{d\omega} \right|_{\omega_0} \\ &+ \frac{1}{2(n_0 - 1)} \left. \frac{d^2n(\omega)}{d\omega^2} \right|_{\omega_0}. \end{aligned} \quad (3.4)$$

Next, we restrict the analysis to the particular but very important case of radially symmetric

optical system, i.e., angular dependent aberrations such as coma or astigmatism are not taken into account, and besides, the amplitude transmission of the pupil aperture should be a radial function. Then Eq. (2) becomes

$$\begin{aligned}
 U(r, z; \Delta\omega) &= 2\pi KA(\Delta\omega)e^{ik_0n_0e\Delta\omega(a_1+a_2\Delta\omega)} \\
 &\times \exp\left\{i\frac{k_0}{2(f_0+z)}\left(1+\frac{\Delta\omega}{\omega_0}\right)r^2\right\} \\
 &\times \int_0^\infty P_0(\rho)e^{i\Phi(\rho)}\exp\left\{-\frac{ik_0}{2f_0}\left(1-\frac{f_0}{f_0+z}\right)\rho^2\right\} \\
 &\times \exp\left\{-\frac{ik_0\Delta\omega}{2f_0}\left(a'_1+a'_2\Delta\omega-\frac{f_0}{\omega_0(f_0+z)}\right)\rho^2\right\} \\
 &\times J_0\left[\frac{k_0}{f_0+z}\left(1+\frac{\Delta\omega}{\omega_0}\right)r\rho\right]\rho d\rho, \tag{4}
 \end{aligned}$$

being $J_0(x)$ the Bessel function of zero order and first kind. So, the image irradiance results as

$$\begin{aligned}
 I(r, z; \Delta\omega) &= |U(r, z; \Delta\omega)|^2 \\
 &= |2\pi KA(\Delta\omega)|^2 \\
 &\times \left|\int_0^\infty P(\rho)\exp\left\{-\frac{ik_0}{2f_0}\left(1-\frac{f_0}{f_0+z}\right)\rho^2\right\}\right. \\
 &\times \exp\left\{-\frac{ik_0\Delta\omega}{2f_0}\left(a'_1+a'_2\Delta\omega-\frac{f_0}{\omega_0(f_0+z)}\right)\rho^2\right\} \\
 &\times J_0\left[\frac{k_0}{f_0+z}\left(1+\frac{\Delta\omega}{\omega_0}\right)r\rho\right]\rho d\rho\left|^2 \tag{5.1}
 \end{aligned}$$

with the amplitude transmittance written as

$$P(\rho) = P_0(\rho)e^{i\Phi(\rho)}. \tag{5.2}$$

Eq. (5.1) is a general result, which provides the irradiance at any point of coordinates (r, z) in the image space. Along the optical axis (where $r = 0$), it becomes

$$\begin{aligned}
 I_0(z; \Delta\omega) &= I(0, z; \Delta\omega) \\
 &= |2\pi KA(\Delta\omega)|^2 \\
 &\times \left|\int_0^\infty P(\rho)\exp\left\{-\frac{ik_0}{2f_0}\left(1-\frac{f_0}{f_0+z}\right)\rho^2\right\}\right. \\
 &\times \exp\left\{-\frac{ik_0\Delta\omega}{2f_0}\left(a'_1+a'_2\Delta\omega-\frac{f_0}{\omega_0(f_0+z)}\right)\rho^2\right\}\rho d\rho\left|^2 \tag{6}
 \end{aligned}$$

Now, we perform the following change of variable: $(\rho/a)^2 = \zeta + 1/2$, which converts any two-dimensional radially symmetric function $P(\rho)$, defined for $0 < \rho < a$, into a one-dimensional function $Q(\zeta)$, which is different from zero only in the interval $-0.5 < \zeta < 0.5$. By expressing the modulus squared in Eq. (6) as the product of two integrals (with integration variables ζ_1 and ζ_2), and by considering centre- and difference-coordinates: $\zeta = (\zeta_1 + \zeta_2)/2$, $\Delta\zeta = \zeta_1 - \zeta_2$, the irradiance along the optical axis can be rewritten as

$$\begin{aligned}
 I_0(z; \Delta\omega) &= |\pi K'A(\Delta\omega)|^2 \\
 &\times \int_{-\infty}^\infty \int_{-\infty}^\infty Q(\zeta + \Delta\zeta/2)Q^*(\zeta - \Delta\zeta/2) \\
 &\times \exp\left\{-i\Delta\zeta\left[\frac{k_0a^2}{2f_0}\left(1-\frac{f_0}{f_0+z}\right) + \frac{k_0a^2\Delta\omega}{2f_0}\right.\right. \\
 &\times \left.\left.\left(a'_1+a'_2\Delta\omega-\frac{f_0}{\omega_0(f_0+z)}\right)\right]\right\}d\zeta d\Delta\zeta, \tag{7}
 \end{aligned}$$

where $K' = Ka^2/2$, and $Q(\zeta)$ is the one-dimensional modified pupil function (obtained from $P(\rho)$ through the change of variable: $\rho = \rho(\zeta)$), which is identically zero outside the interval $-1/2 < \zeta < 1/2$. For this reason the integration limits extend to $\pm\infty$. By taking into account the WDF definition (see e.g. [1,2]), Eq. (7) can be rewritten in terms of the WDF as

$$\begin{aligned}
 I_0(z; \Delta\omega) &= |\pi KA(\Delta\omega)|^2 \int_{-\infty}^\infty W_Q[y(z; \Delta\omega), \zeta] d\zeta \\
 &= |\pi K'A(\Delta\omega)|^2 \\
 &\times \int_{-\infty}^\infty W_Q\left[\frac{k_0a^2}{2f_0}\left(\frac{z-f_0\Delta\omega/\omega_0}{z+f_0} + a'_1\Delta\omega + a'_2\Delta\omega^2\right), \zeta\right] d\zeta, \tag{8}
 \end{aligned}$$

which states that the on-axis irradiance for each value of z is given by the spatial frequency projection of the WDF associated with the modified pupil function $Q(\zeta)$ along vertical slices in the phase-space (y, ζ) . The value of the y -coordinate depends on the defocus distance z , the dispersion properties of the lens material, and the spectral content $\Delta\omega$ of the light beam. The relationship between these phase-space locations and the defocus distance z is $y(z; \Delta\omega)$, as can be seen in Eq.

(8). This expression becomes infinity for $z = -f_0$ (the location of the pupil aperture), but the approximations involved to derive Eqs. (2)–(8) are not valid for points too close to the pupil plane. It is clear from Eq. (8) that, for increasing values of z , the locations of the vertical phase-space slices shift from the centre of the WDF display, so diminishing the on-axis irradiance. Besides, as stated by

Eq. (8), the image irradiance is also affected by the light spectral content given by $A(\Delta\omega)$, which is to be analysed in the examples of the following section.

Finally, we analyse how the dispersion affects the presence of each frequency at a given location z . The relationship $y = y(\Delta\omega)$ (from Eq. (8)) can be expressed as

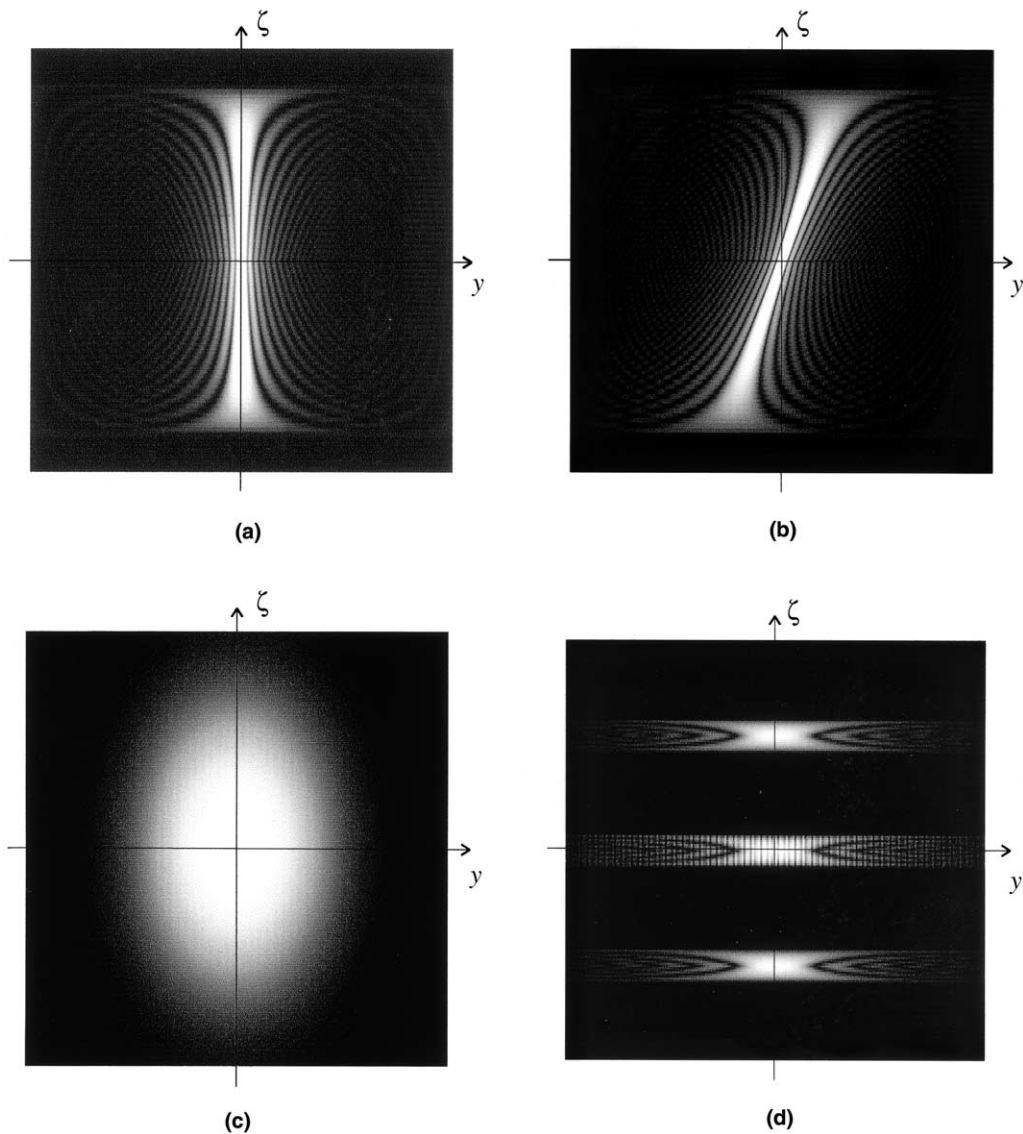


Fig. 2. Gray-level picture of the WDF associated with a rectangle function as reduced pupil function of: (a) uniform circular aperture, (b) quartic phase pupil function, (c) hyper-gaussian transmission function, (d) annular aperture.

$$y(\Delta\omega) = \left(\frac{k_0 a^2}{2f_0} a'_2\right) \Delta\omega^2 + \left(\frac{k_0 a^2}{2f_0}\right) \times \left(a'_1 - \frac{f_0}{\omega_0(z+f_0)}\right) \Delta\omega + \frac{k_0 a^2}{2f_0} \frac{z}{z+f_0}. \tag{9}$$

This is a shifted parabolic curve: its second order coefficient is related with the second order dispersion parameter, while the linear coefficient depends on the first order dispersion parameter. The independent coefficient only depends on the geometric lens properties and the defocus distance z . For a small second order dispersion ($a'_2 \cong 0$), Eq. (9) can be approximated as

$$y(\Delta\omega)|_{a'_2 \cong 0} = \left(\frac{k_0 a^2}{2f_0}\right) \left(a'_1 - \frac{f_0}{\omega_0(z+f_0)}\right) \Delta\omega + \frac{k_0 a^2}{2f_0} \frac{z}{z+f_0}. \tag{10}$$

The slope of this line contains both, the first order dispersion and the geometric parameters, while the interception-to-zero term involves only the latter. In order to illustrate the behaviour of the optical system, we consider a circular uniform aperture having associated a WDF which is displayed as a gray-level picture in Fig. 2(a). If the illumination spectral width $\Delta\omega$ increases, the condition $y = 0$ (corresponding to maximum irradiance) is found for larger values of z , that is the well-known chromatic focal shifting. Other effect which can be visualised from Eq. (10) is that, at the focal point ($z = 0$), the interception-to-zero term becomes zero and the absolute value of the slope has its minimum. Thus, in order to get most of the spectral components be present at the focal point, it is desirable to have a smoother WDF variation along the y -axis, as compared with that shown in Fig. 2(a), taking into account that the on-axis irradiance results by adding the WDF ζ -values. In the next section, pupil apertures producing this smooth-varying effect are to be analysed.

3. Tolerance to defocus in the polychromatic case

In order to illustrate the proposed approach, we analyse the imaging properties of four different

pupil apertures under polychromatic illumination, namely, a uniform aperture, an annular aperture, a quartic phase pupil and a quartic phase pupil and a hyper-gaussian transmission function, which are given by the following expressions:

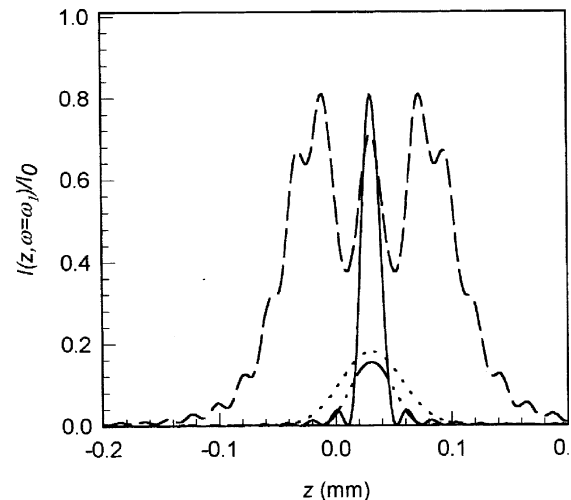
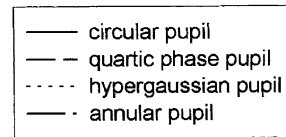
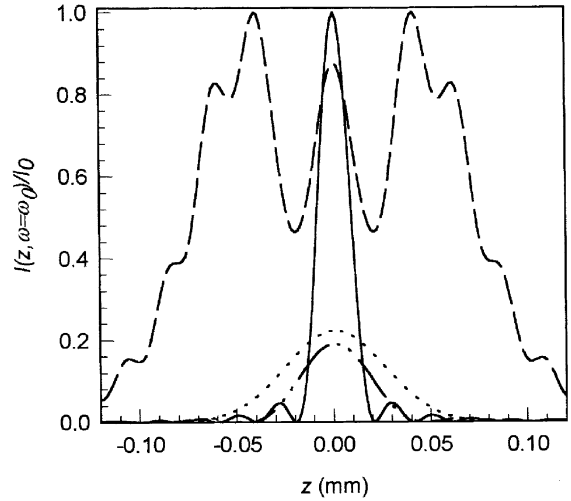


Fig. 3. Irradiance curves $I_0(z; \Delta\omega)$ for two different spectral frequencies: $\omega = \omega_0 = 3.0381E15$ Hz ($\Delta\omega = 0$) and $\omega = 1.562 \omega_0$ ($\Delta\omega > 0$).

$$P(\rho) = \text{circ}(\rho/a), \tag{11.1}$$

$$P(\rho) = \text{circ}(\rho/a) - \text{circ}(\rho/\varepsilon a), \tag{11.2}$$

$$P(\rho) = \text{circ}(\rho/a) e^{-i\pi\alpha((\rho/a)^4 - (\rho/a)^2 + 0.25)}, \tag{11.3}$$

$$P(\rho) = \text{circ}(\rho/a) e^{-2\pi\gamma((\rho/a)^2 - 0.5)^2}. \tag{11.4}$$

The values of the involved pupil parameters were selected as $\alpha = 10$, $\gamma = 10$ and $\varepsilon = 0.75$. The WDF

displays corresponding to these apertures are illustrated in Fig. 2. The spectral content of the light beam was assumed to be characterised by a gaussian function of the form

$$A(\Delta\omega) = e^{-(\Delta\omega/\delta\omega)^2}, \tag{12}$$

being $\delta\omega$ the mean spectral width. The value of ω_0 was chosen as $\omega_0 = 3.0381\text{E}15$ Hz, or equivalently, $\lambda_0 = 620$ nm. The irradiance curves $I_0(z; \Delta\omega)$, obtained from Eq. (8) for: $\Delta\omega = 0$ (or,

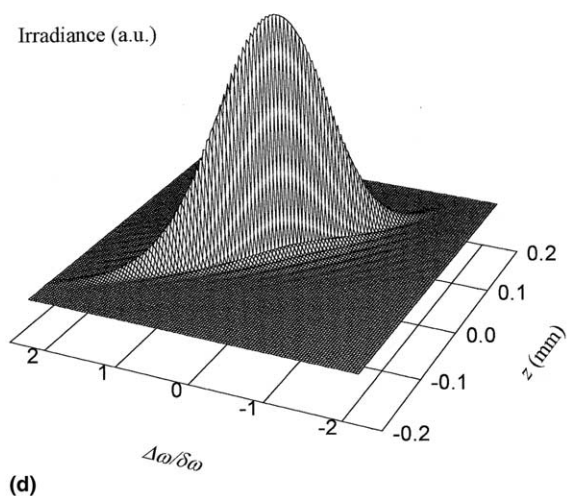
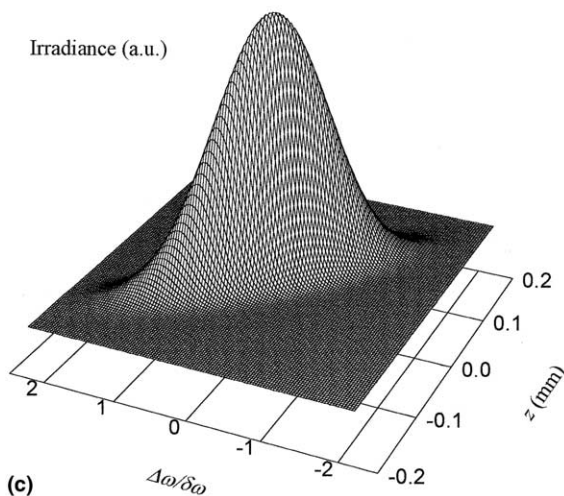
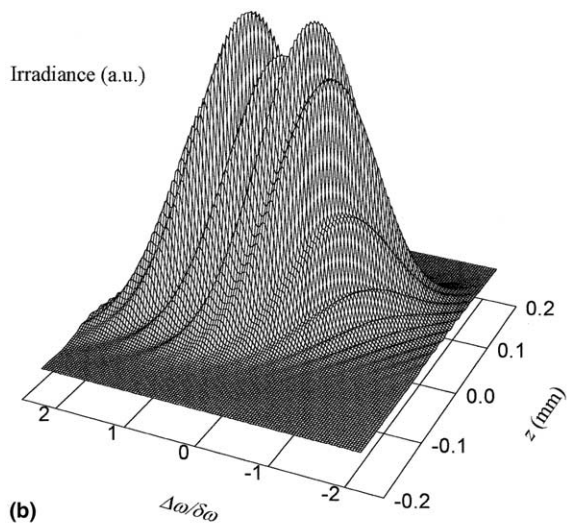
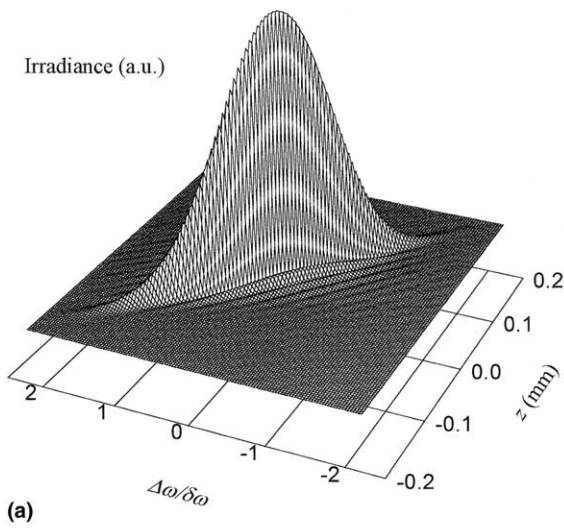


Fig. 4. Three-dimensional displays of the irradiance vs. defocusing and spectral frequencies for: (a) circular aperture, (b) quartic phase pupil, (c) hyper-gaussian transmission function, (d) annular aperture.

$\omega = \omega_0$) and $\Delta\omega > 0$ ($\omega = 1.562\omega_0$, $\lambda = 400$ nm), are plotted in Fig. 3. It can be clearly seen the different focusing performances of the several apertures and the expected shift of the irradiance maximum for $\omega \neq \omega_0$. It is interesting to visualise the irradiance distributions for the four analysed cases in the spatial–spectral domain ($z, \Delta\omega$), which are shown in Fig. 4 as three-dimensional displays and in Fig. 5 as gray-level pictures. Finally, the intensity distributions, for varying defocus integrated for all spectral frequencies present in the illuminating beam, are shown in Fig. 6. From these results, it can be seen the frequency depend-

dence of the focal point that originates the axial chromatic aberration. For an ideal optical system, the irradiance maxima for each frequency would be located at the same point on the optical axis. Besides, if this system is tolerant to defocusing, then the whole irradiance distribution varies slowly with z . From the results illustrated in Figs. 3–6, it can be concluded that both, the quartic phase function and the hyper-gaussian function, have associated a broader $\Delta\omega$ region in $z = 0$, and show a smoother variation for $z \neq 0$ than that corresponding to the uniform and annular apertures.

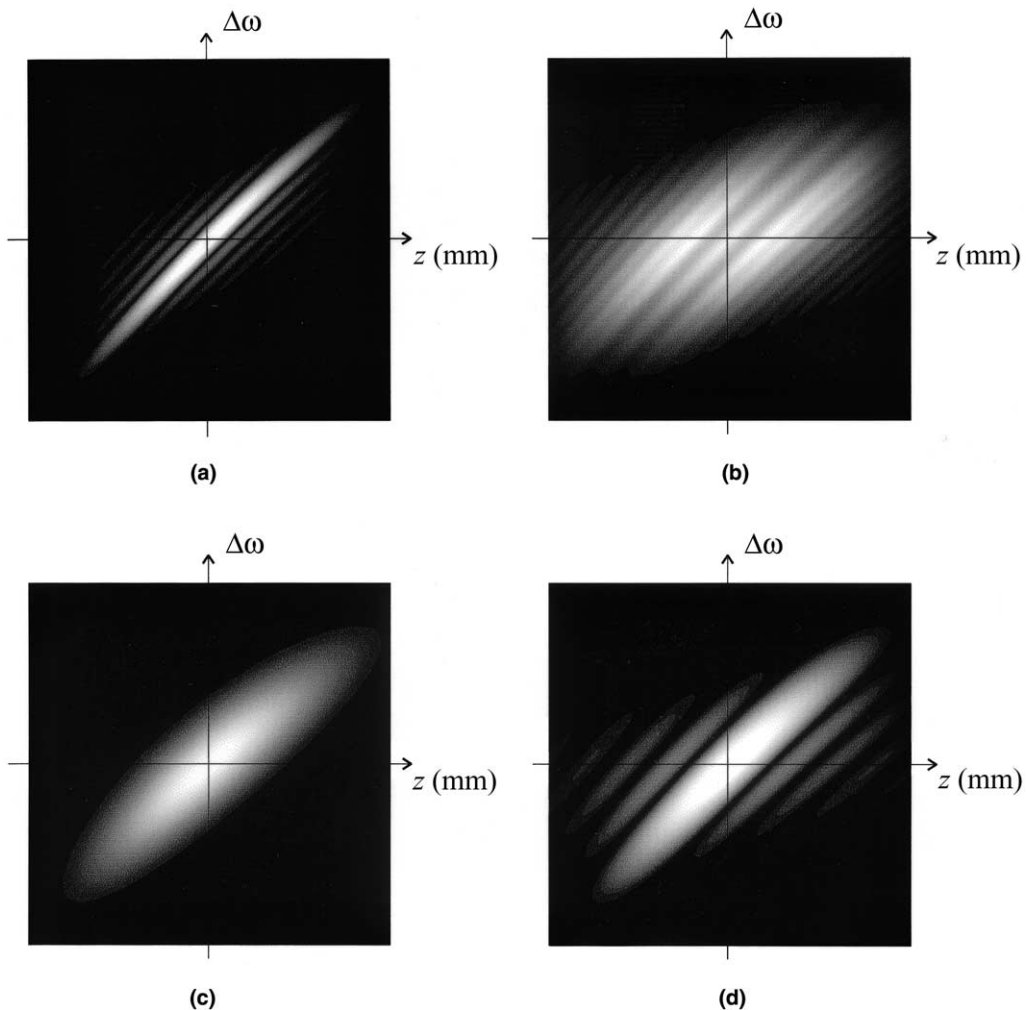


Fig. 5. Gray-level pictures of the displays shown in Fig. 4.

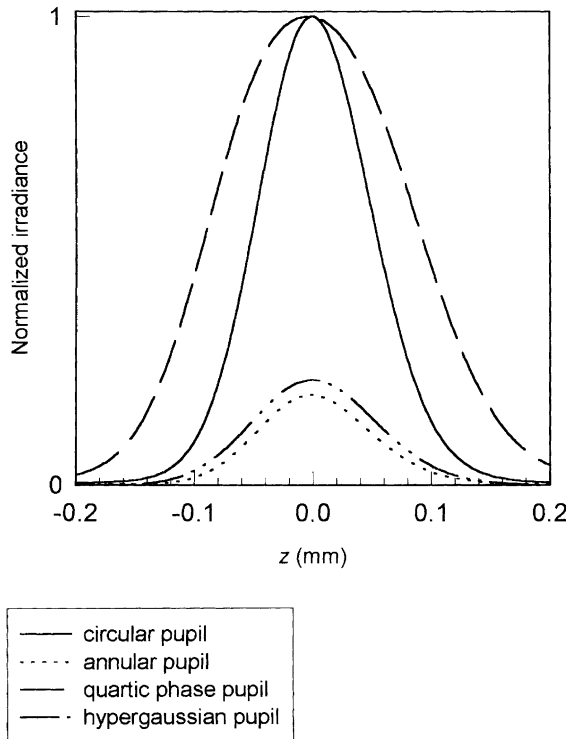


Fig. 6. Irradiance curves vs. defocusing, integrated for all spectral frequencies, for the four analysed pupil functions.

4. Conclusions

In this paper we extend the treatment of optical imaging systems by using the WDF to the case of broadband or polychromatic illumination. The on-axis irradiance in the image space was found as proper spatial frequency projections of a two-dimensional WDF associated with a reduced pupil

aperture. A relationship was derived which links the three main involved parameters, namely, the defocus distance, the spectral frequency and the material dispersion. Finally, the approach was illustrated by comparing the imaging behaviour of four different apertures. From the WDF displays, it can be visualised the better performance to defocusing of two of the apertures: the hypergaussian transmission function and the quartic phase mask.

References

- [1] M.J. Bastiaans, *Opt. Commun.* 25 (1978) 26.
- [2] H.O. Bartelt, K.-H. Brenner, A.W. Lohmann, *Opt. Commun.* 32 (1980) 32.
- [3] A. Papoulis, *J. Opt. Soc. Am.* 64 (1974) 779.
- [4] H. Bartelt, J. Ojeda-Castañeda, E.E. Sicre, *Appl. Opt.* 23 (1984) 2693.
- [5] J. Ojeda-Castañeda, P. Andrés, E. Montes, *J. Opt. Soc. Am. A* 4 (1987) 313.
- [6] J. Ojeda-Castañeda, L.R. Berriel-Valdos, E. Montes, *Appl. Opt.* 27 (1988) 790.
- [7] L.V. Bourimborde, W.D. Furlan, E.E. Sicre, *J. Mod. Opt.* 38 (1991) 1685.
- [8] W.D. Furlan, G. Saavedra, J. Lancis, *Opt. Commun.* 96 (1993) 208.
- [9] E.R. Dowski Jr., W.T. Cathey, *Appl. Opt.* 34 (1995) 1859.
- [10] D. Zalvidea, M. Lehman, S. Granieri, E.E. Sicre, *Opt. Commun.* 118 (1995) 207.
- [11] G. Saavedra, W.D. Furlan, E. Silvestre, E.E. Sicre, *Opt. Commun.* 139 (1997) 11.
- [12] A.R. FitzGerrell, E.R. Dowski Jr., W.T. Cathey, *Appl. Opt.* 36 (1997) 5796.
- [13] D. Zalvidea, E.E. Sicre, *Appl. Opt.* 37 (1998) 3623.
- [14] D. Zalvidea, C. Colautti, E.E. Sicre, *J. Opt. Soc. Am. A* 17 (2000) 867.